A NOVEL OPTIMIZATION PLATFORM AND ITS APPLICATIONS TO THE TRIUMF ENERGY RECOVERY LINAC*

C. Gong and Y. C. Chao
TRIUMF, 4004 Wesbrook Mall, Vancouver V6T 2A3, Canada

Abstract

A software platform for global optimization was developed to study the TRIUMF Energy Recovery Linac. The platform is parallel capable and allows for combinations of accelerator modeling tools such as MADX and Genesis. Many parameters are coupled, including RF parameters which are shared for all linac passes. The platform can study dynamic relationships between different processes, a practice not easily performed with standalone optimization. Tradeoffs are presented to give insights on how objectives are related and the repercussions of design decisions.

INTRODUCTION

The TRIUMF E-linac is a 50 MeV, 10 mA average current CW driver for rare isotope beams (RIB). The E-linac can be upgraded to an Energy Recovery Linac (ERL) for simultaneous ERL and RIB operations.

The design of the upgrade is complicated. Many parameters are coupled, including RF parameters which are shared between three beams (RIB pass and two ERL passes). Our goals are:

- Create a computational platform for multiobjective optimization (MOO), capable of massively parallel computation.
- Capable of using different modeling tools, or engines, in combination to produce global models of machines.
- Use the platform to set up a global ERL model.
- Use the platform to study the physics of the TRIUMF ERL.
- Create a baseline from optimization results, complete with layout coordinates and optics requirements.

More details on the capabilities of the platform can be found in [1, 2]. The complete platform design and implementation can be found in [3], with a description of MOO.

OPTIMIZATION METHOD

Objectives and constraints used in the optimization are

- Maximize gain, therefore FEL power.
- Energy recovery: $E_{dmp} = E_{in}$ =7.5 MeV, or equivalently, $p_{dmp} = p_{in}$ =7.5 MeV/c - dump energy same as injection energy.
- $\sigma_x \leq 3$ mm, $\sigma_y \leq 3$ mm - minimize beam loss via beam scraping by restricting transverse beam size everywhere.
- $\sigma_{x,EDBT} \leq 3$ mm, $\sigma_{y,EDBT} \leq 3$ mm - constrain beam size in the dump section EDBT. This is complicated by the large energy spread δ obtained from lasing and deceleration, which is converted to beam size by the EDBT dipole. This constraint overlaps with the previous, but is listed again for emphasis.
- beam loss $\leq 10^{-5}$ - lasing creates a momentum tail which can cause beam loss in the return arc.
- $\sigma_{x,dmp} = 7$ mm, $\sigma_{y,dmp} = 7$ mm - blow up beam at the dump to reduce radiation heating.
- $\alpha_x = \alpha_y = \eta_{x'} = 0$ at both arc centers - look for designs with arc symmetries in β_x, β_y, and η_x. Symmetries make tuning easier. The layout of the arc optics is symmetric to accommodate these conditions. η_y is zero everywhere and does not need to be considered.
- Maximize E_{RIB} - high energy is desired for RIB transport.

Free parameters in the optimization are:

- RF phases and amplitudes (four independent cavities)
- Drift lengths (25 cm minimum separation between elements to support diagnostics)
- Quad gradients (upper limit set by existing TRIUMF magnet designs)
- Chicane dipoles bend angle

The main linac geometry is designed and not subject to optimization. Care is also taken to make sure the ERL fits in the TRIUMF E-hall.

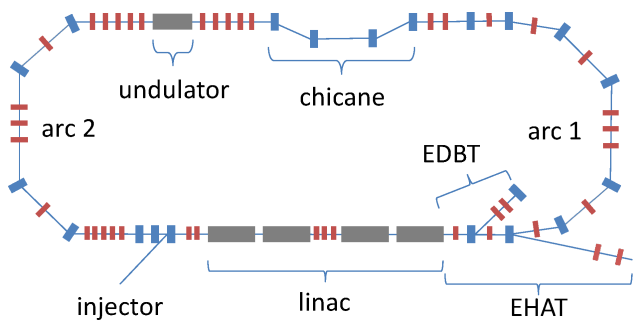

Figure 1: Dual ERL-RIB layout.

Layout of the ERL is shown in Fig. 1. Modeling of the machine starts at the linac. After acceleration an RF separator kicks the ERL beam into the recirculation loop. The beam lases and is then decelerated by a second pass. The energy recovered beam is kicked to EDBT for disposal. The RIB pass is modeled as well, with the RF separator kicking the beam into RIB transport EHAT.

Components of the ERL are modeled by a combination of engines: MADX, DIMAD, Genesis, and the Empirical Model (EM) [4]. EM is a TRIUMF code for modeling cavities. The optimization platform handles all transitions between engines and distribution of work on parallel clusters.

* Work supported by Natural Sciences and Engineering Research Council of Canada and National Research Council of Canada

ISBN 978-3-95450-136-6

Engines can be easily switched because the platform treats them as independent modules.

RESULTS

Most plots shown in this section represent either the optimization population, or a subset of the population. Each point in the plots should be interpreted as an instance of the ERL, i.e. a particular machine design created by the optimization platform.

The RF can have a significant impact on bunch compression and therefore the gain. Figure 2 shows the effects of the acceleration phase ϕ_1 on the gain. The data forms the typical shape of the RF curve, demonstrating the important role of RF in shaping the bunch for compression and lasing. Note that in EM convention, phases denote when the bunch centroid is at the cavity entrance. 335°/155° represents the RF crest/trough. Figure 2 shows the best bunch compression occurs when the beam is accelerated several degrees before crest.

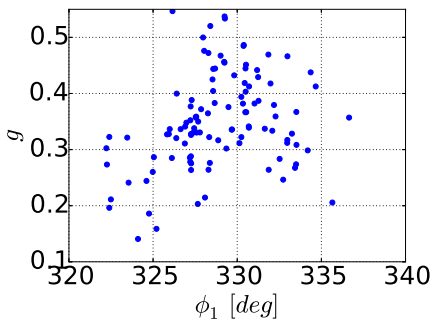

Figure 2: FEL gain vs acceleration phase ϕ_1. Slices made on parameters at the undulator entrance: $\beta_x \leq 2$ m, $\beta_y \leq 2$ m, $-0.5 \leq \alpha_x \leq 0.5$, and $0.5 \leq \alpha_x \leq 1.5$. These slices are centered around the optimal transverse matching conditions for the undulator (Eq. (1)) to isolate longitudinal effects. The solution set encompasses physics of the linac, arc transport, and lasing. No single simulation tool can provide all the physics modeling necessary.

We follow the evolution of the energy spread δ in the machine. δ increases as a result of lasing (Fig. 3), by several 10^{-3}. The larger δ can cause problems for the return transport, where arc dipoles can convert δ into beam size, potentially resulting in beam loss.

δ also increases significantly after linac pass 2 due to anti-damping (Fig. 4). This causes problems for transport in the dump section EDBT, where again δ can be converted into beam size and beam loss. Notice that δ increases by an order of magnitude before and after acceleration.

Lasing also induces non-Gaussian effects in the bunch. Figure 5 shows the distribution of bunch particles' energy deviation after lasing. A slight tail can be observed. Its effects need to be tracked in the second transport arc, where the tail can be turned into beam size by the dipoles and cause beam loss.

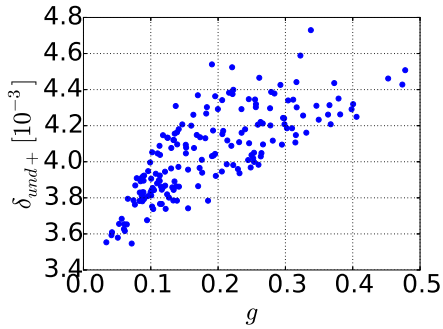

Figure 3: Increase in δ due to lasing.

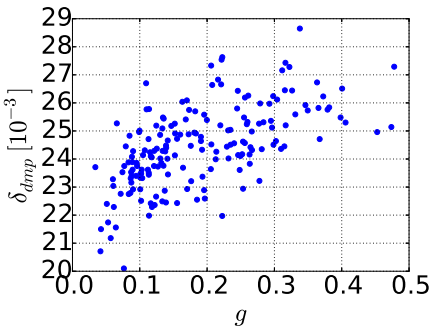

Figure 4: Effects of gain on δ and beam disposal.

In addition to constraining beam sizes σ_x and σ_y, we also require beam loss $\leq 10^{-5}$ through particle tracking to observe effects of the momentum tail.

Figure 6 shows maximum horizontal and vertical beam sizes in the return arc. Blue solutions satisfy beam size constraints $\sigma_x \leq 3$ mm and $\sigma_y \leq 3$ mm. Red solutions satisfy both beam size constraints and beam loss $\leq 10^{-5}$. The red solutions are a subset of the blue. The momentum tail tightens the maximally allowed beam sizes to $\sigma_x \leq 2.9$ mm and $\sigma_y \leq 2.8$ mm.

Figure 7 shows the importance of the RF deceleration phase ϕ_2. Both momentum p and energy spread δ are greatly affected. The closer the bunch enters the linac on-crest, the greater deceleration it experiences, but this leads to a decrease in RF slope and therefore less control of δ. This coupling leads to a tradeoff.

Figure 8 shows the tradeoff, or Pareto front, between energy recovered p and δ at the dump. For energy recovery,

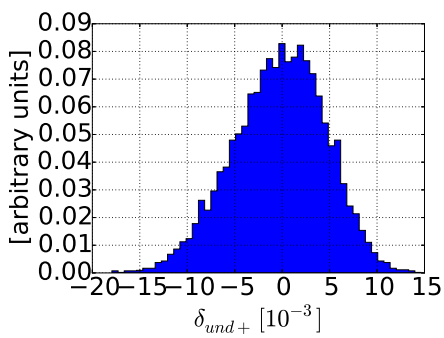

Figure 5: Energy deviation of particles in bunch after lasing.

ISBN 978-3-95450-136-6

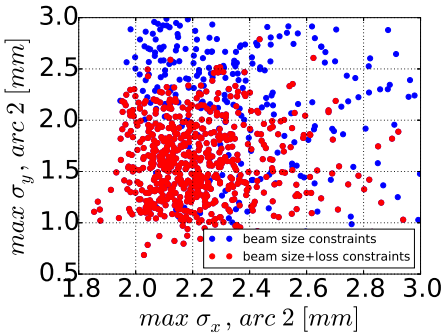

Figure 6: Tracking beam loss after lasing.

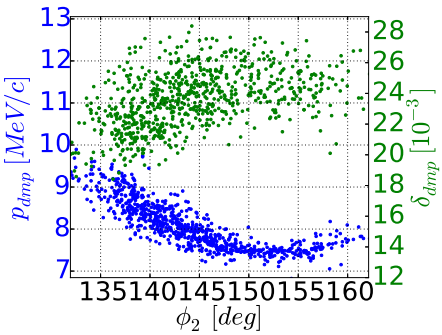

Figure 7: Effects of ϕ_2.

we wish to move left towards the vertical red line, which shows the desired injection $p = 7.5$ MeV/c. At this momentum only a 0.021 minimum δ_{dmp} is achievable. To lower δ_{dmp}, we wish to move to the right. The two parameters are fighting against each other because they are both coupled to ϕ_2. If δ at the dump becomes an issue, it is possible to sacrifice energy recovery to achieve smaller δ.

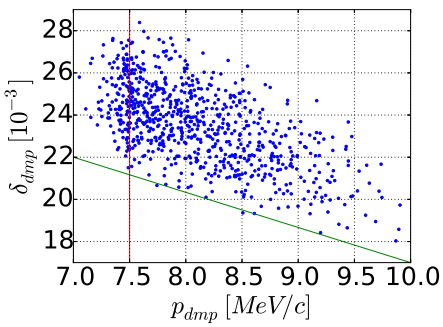

Figure 8: Pareto front between energy recovered momentum p_{dmp} and energy spread at dump δ_{dmp}.

The theoretical matching conditions for the undulator are given by [5]. Horizontally the undulator resembles a drift so we want the incoming beam to be focusing and form a symmetric waist at the center. Vertically, the B-field is sinusoidal with $B_y \approx B \cos k_u z$, where $k_u = 2\pi/4$ cm is the undulator wavenumber. The field can be averaged over the undulator period λ_u to create a section of constant focusing strength $K/(\sqrt{2}\gamma_r \lambda_u)$ where $K = .7$ is the undulator parameter and $\gamma_r \approx 90$ is the Lorentz factor of the bunch. Thus we would

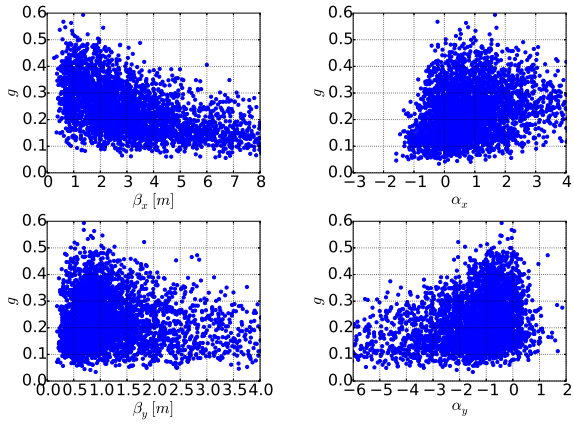

Figure 9: Undulator matching conditions from optimization match well with Eq. (1).

like a coasting beam. The matching parameters are

$$\begin{aligned} \beta_{x,match} &= Z_R + (L_u^2/4Z_R) = 1 \text{ m} \\ \alpha_{x,match} &= L_u/(2Z_R) = 1 \\ \beta_{y,match} &= \sqrt{2}\gamma_r/(K k_u) \approx Z_R = .5 \text{ m} \\ \alpha_{y,match} &= 0 \end{aligned} \tag{1}$$

where $Z_R = .5$ m is the Rayleigh length and $L_u = 1$ m is the undulator length. Optimization results supports these conditions (Fig. 9).

BASELINE

An ERL baseline is chosen from the optimization population. Important values are displayed in Table 1.

Table 1: ERL Engine Topology

Parameter	Value
Gain	0.5 m^{-1}
Initial momentum	7.5 MeV
EDBT momentum	7.7 MeV
σ_x	$\leq$ 3 mm everywhere
σ_y	$\leq$ 3 mm everywhere
EDBT energy spread	0.029
EDBT max σ_x	3.0 mm
EDBT max σ_y	1.9 mm
Dump σ_x	5.5 mm
Dump σ_y	6.0 mm
Beam loss	$\leq 10^{-5}$

The design has a gain of 0.5 m^{-1}. This is near the top of the optimization search space for gain and satisfies our maximize lasing objective.

The EDBT max σ_x is within our beam size constraint, demonstrating that energy spread is contained and should not be an issue.

Further physics and baseline results can be found in [3].

ISBN 978-3-95450-136-6

REFERENCES

[1] C. Gong and Y.C. Chao, "A New Platform for Global Optimization," IPAC12, New Orleans, 2012.

[2] C. Gong and Y.C. Chao, "The TRIUMF Optimization Platform and Application to the E-Linac Injector," ICAP12, Rostock, 2012.

[3] C. Gong, "A Novel Optimization Platform and Its Applications to the TRIUMF Energy Recovery Linac," PhD Dissertation, University of British Columbia, 2015.

[4] Y.C. Chao et al., "Low-Beta Empirical Models used in Online Modeling and High Level Applications," IPAC11, San Sebastian, 2011.

[5] Y.C. Chao, "Wiggler Parameters and Matching Conditions," Unpublished TRIUMF note, 2014.

ISBN 978-3-95450-136-6